

# Benzoin Radicals as Reducing Agent for Synthesizing Ultrathin Copper Nanowires

Fan Cui,<sup>†,‡,∇</sup> Letian Dou,<sup>†,‡,∇</sup> Qin Yang,<sup>†</sup> Yi Yu,<sup>†,∇</sup> Zhiqiang Niu,<sup>†,‡,∇</sup> Yuchun Sun,<sup>†</sup> Hao Liu,<sup>†</sup> Ahmad Dehestani,<sup>‡</sup> Kerstin Schierle-Arndt,<sup>‡</sup> and Peidong Yang<sup>\*,†,‡,∇,#</sup>

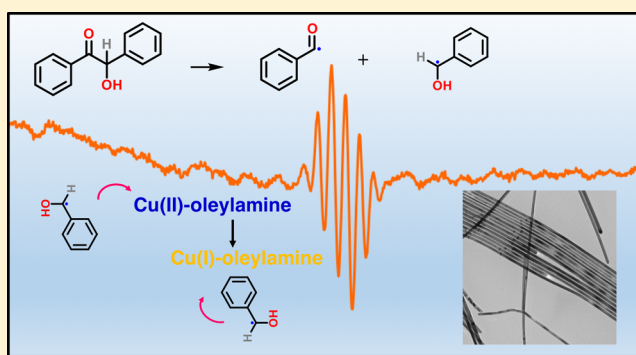
<sup>†</sup>Department of Chemistry, <sup>#</sup>Department of Materials Science and Engineering, University of California at Berkeley, Berkeley, California 94720, United States

<sup>‡</sup>California Research Alliance (CARA), BASF Corporation, Berkeley, California 94720, United States

<sup>∇</sup>Materials Sciences Division, Lawrence Berkeley National Laboratory, Berkeley, California 94720, United States

## S Supporting Information

**ABSTRACT:** In this work, we report a new, general synthetic approach that uses heat driven benzoin radicals to grow ultrathin copper nanowires with tunable diameters. This is the first time carbon organic radicals have been used as a reducing agent in metal nanowire synthesis. *In-situ* temperature dependent electron paramagnetic resonance (EPR) spectroscopic studies show that the active reducing agent is the free radicals produced by benzoin under elevated temperature. Furthermore, the reducing power of benzoin can be readily tuned by symmetrically decorating functional groups on the two benzene rings. When the aromatic rings are modified with electron donating (withdrawing) groups, the reducing power is promoted (suppressed). The controllable reactivity gives the carbon organic radical great potential as a versatile reducing agent that can be generalized in other metallic nanowire syntheses.



## INTRODUCTION

One-dimensional metal nanowires (NWs) have many unique properties different from their bulk form. They have been demonstrated as crucial building blocks in various applications such as electronics,<sup>1</sup> optics,<sup>2</sup> catalysts,<sup>3</sup> and sensors.<sup>4</sup> In particular, metal NWs have been extensively studied as high performance transparent conductors.<sup>5</sup> Copper's high earth abundancy and intrinsic conductivity place it among the most popular materials in the field of NW mesh electrodes. Copper NWs have been successfully synthesized, mainly via solution chemistry, by a number of groups. The general method is to reduce a copper ion/ion complex in the presence of capping ligands with efficient reducing agents including primary amine,<sup>6</sup> glucose,<sup>7</sup> ascorbic acid,<sup>8</sup> hydrazine,<sup>9</sup> silanes,<sup>10</sup> or via catalyst-assisted methods.<sup>11</sup> One-dimensional NW growth can also be achieved by screw dislocation.<sup>12</sup> The quality of the Cu NWs synthesized is usually the key factor in achieving high performance NW devices. Monodispersity, high aspect-ratio, diameter controllability, and low synthetic costs are always desired. To gain better control over the morphology of the synthesized NWs, it is critical that the nucleation rate is precisely controlled,<sup>11</sup> and thus, the choice of reducing agent should be taken into great consideration.

Here, for the first time, we introduce benzoin free radicals as a general and controllable reducing agent for the synthesis of Cu NWs. This method can easily produce monodispersed, size-

controllable Cu NWs with diameter ranging from ~36 to ~18 nm. The reaction mechanism was investigated using *in situ* EPR and carbon radical species are identified as the effective reductants. Moreover, we demonstrate the reactivity tunability by introducing electron-donating/electron-withdrawing functional groups on benzoin.

## RESULTS AND DISCUSSION

The synthesis of Cu NWs is summarized in Figure 1a. Copper chloride, which is dissolved in oleylamine, can be slowly reduced under heating condition in the presence of benzoin, and eventually form one-dimensional NWs. Oleylamine here acts as the sole solvent as well as surface ligands. In this reaction, we believe that benzoin acts as the key reducing agent, which reduces Cu(II) species to Cu(I) and then to Cu metal. Benzoin is commonly used as a photoinitiator in polymerization,<sup>13</sup> but its application in colloidal nanomaterial synthesis is rarely documented,<sup>14</sup> even more rare so under heating conditions. It is well-known that, under UV illumination, benzoin produces two radicals via  $\alpha$ -cleavage, in which the carbon-carbon  $\sigma$  bond undergoes homolytic bond cleavage upon absorption of light.<sup>15</sup> We hypothesize here that under heating condition, benzoin behaves in a similar manner. At

Received: November 17, 2016

Published: January 31, 2017

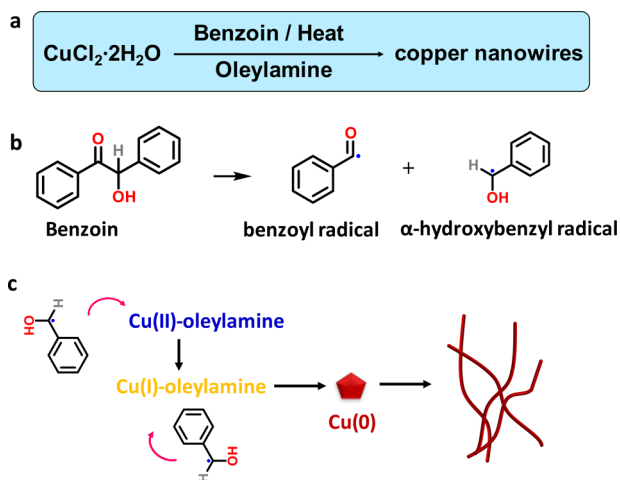


**Figure 1.** (a) Overall reaction scheme of Cu NW synthesis using benzoin as reducing agents; (b) heat induced radical generation from benzoin; (c) proposed mechanism of Cu complex reduction via benzoin radicals and one-dimensional NW growth.

elevated temperature, it yields radicals in an inert environment and the resulting radicals can act as efficient electron donors. The detailed proposed reaction mechanism is shown in Figure 1 panels b and c. When benzoin is heated, it decomposes into two radical segments, benzoyl radical and  $\alpha$ -hydroxybenzyl radical. In an air-free atmosphere, the radicals are relatively stable due to the conjugation of benzene ring, and thus have a long enough lifetime to reduce metal complex in solution. The reduction of a copper complex takes place in two steps: at lower temperature Cu(II) species are first reduced to Cu(I) which is indicated by the disappearing blue color fingerprint; then at higher temperature, Cu(I) complexes are further reduced to Cu(0). With oleylamine as the coordinating surfactants, the

copper nucleation is known to favor a five-fold-twinned structure. With (100) facets selectively protected by amine groups, newly formed copper metal preferentially deposits onto the (111) surfaces, promoting one-dimensional growth.<sup>11</sup>

The morphologies of the product are examined by scanning electron microscope (SEM) and transmission electron microscope (TEM) as shown in Figure 2a,b. The majority of the products are uniform NWs with a minimum portion of nanoparticles. Such NWs have a length of up to 20  $\mu\text{m}$ , and a diameter of  $18.5 \pm 3.5$  nm. The detailed structure of the Cu NWs is studied using high resolution (HR) TEM and X-ray diffraction (XRD). The NW has the five-fold twinned structure, which consists of five face centered cubic (FCC) single crystalline units. Figure 2c shows the HRTEM image taken when the incident electron beam is perpendicular to one of the side facets. A clear Moiré pattern is observed in the center of the NW, which corresponds to the overlap between the upper single unit and the underlying two units as drawn in the inset.<sup>11</sup> Figure 2d shows the XRD pattern of the as-made Cu NWs. The wires adopt the common FCC pattern. The clean pattern indicates that the products are pure from copper oxides. The inset demonstrates the overall microstructure of the 5-fold twinned Cu NW, with {100} facets as side surfaces and [110] being the growth direction. This structure has been well documented within oleylamine modulated Cu NW syntheses.<sup>6b,10,11</sup>

The diameter of the as-grown Cu NWs can be readily tuned by changing reaction temperatures. We observed that with higher reaction temperature, the NWs synthesized are of a smaller diameter (Figure S1). Figure 2e summarizes the diameter distribution of Cu NWs grown under different temperatures. The averaged NW diameter is increased from 18.5 nm with the reaction temperature of 190  $^{\circ}\text{C}$ , to 23.0 nm with 180  $^{\circ}\text{C}$  and to 36.2 nm with 165  $^{\circ}\text{C}$ . The logic behind the

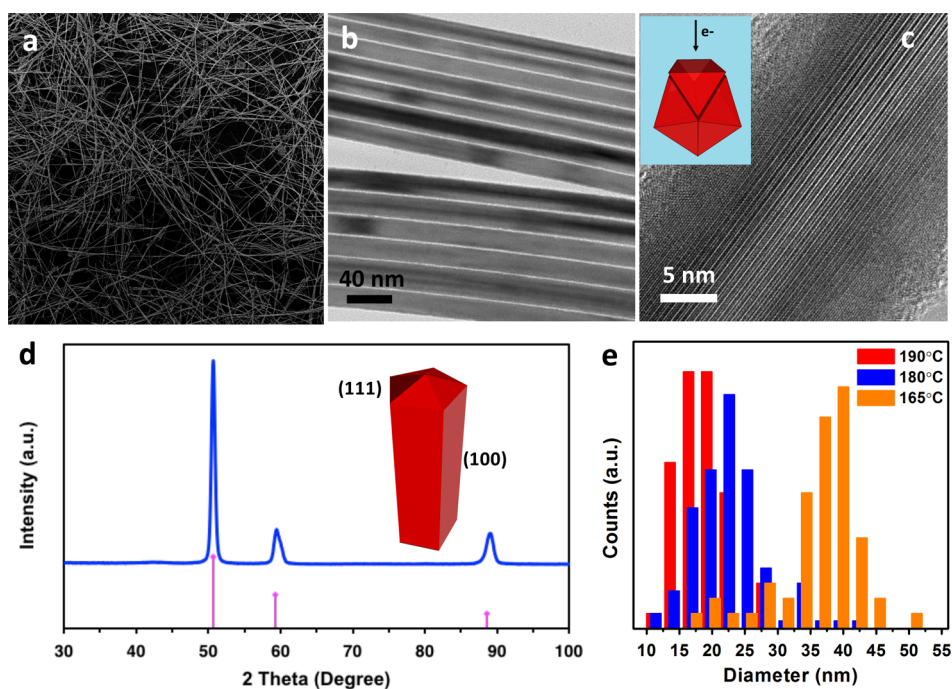


**Figure 2.** (a) SEM, (b) TEM, and (c) HRTEM images of as-synthesized Cu NWs at 190  $^{\circ}\text{C}$ . (d) XRD pattern of as made Cu NWs, inset is a schematic representation of the NW's microstructure. Pink lines are the standard XRD pattern of FCC copper. (e) Diameter distribution of Cu NWs synthesized at 190  $^{\circ}\text{C}$  (red), 180  $^{\circ}\text{C}$  (blue), and 165  $^{\circ}\text{C}$  (orange).

diameter control can be explained by close examination of the nucleation stage. At a higher temperature, the reduction of the Cu complex is faster, leading to a faster nucleation and thus more nucleation sites at the same time frame. Considering that the precursor concentration is kept the same for all experiments, more nucleation sites imply smaller volume for each nucleates, which later will grow into thinner NWs.

To investigate benzoin's role as a reducing agent, we carried out a series of control experiments with benzoin-like chemicals, and the results are summarized in Table 1. Benzaldehyde,

**Table 1. Summary of Reducing Power of Benzoin and Its Similar Structures toward Cu(II) Reduction**

Reducing agent used	Reactivity toward Cu(II)	Comments
	Yes	
	No	
	No	
	No	
	No	R = CH <sub>3</sub> -, CH <sub>3</sub> CH <sub>2</sub> -
	No	
	Yes	X = CH <sub>3</sub> O-, CH <sub>3</sub> -, Cl, F-. F- can slightly react above 200 °C

which is the main byproduct of benzoin's decomposition,<sup>14</sup> shows no activity toward the reduction of copper salt at the condition of interest. Benzoin esters are also tested under similar conditions. Despite the fact that benzoin esters exhibit similar behavior and activity when used as a photoinitiator,<sup>13</sup> no reactivity toward copper reduction is observed here. This suggests that the actual reductants are probably the  $\alpha$ -hydroxybenzyl radicals, rather than its benzoyl counterpart. Another interesting observation is that, when we attach one Cl atom to the aromatic ring (4-chlorobenzoin), again no reduction of copper happens. This is probably because the asymmetrical structure makes homolytic bond cleavage no longer favorable, and thus radicals are not among the major products. This further implies the radical-involving nature of this reaction.

To further understand the proposed radical-involving mechanism, in situ temperature-dependent electron paramagnetic resonance (EPR) spectroscopy is used to track the reduction progress. EPR is a spectroscopic technique that detects species with unpaired electrons, and is informative

toward reactions involving free radicals and/or active metal complexes. In our study, we simulate the typical reaction in a vacuum sealed quartz tube and follow the evolution of the reactants' EPR signals. Similar to the process for the Schlenk tube reaction, the reactants were first mixed and then left at room temperature (RT) for 2 h before being slowly heated to 170 °C, and then left to react for another 3 h. Simultaneously, EPR responses of the solution were acquired at different time/temperature intervals.

The results of the EPR measurements are shown in Figure 3. The first spectrum (blue) in Figure 3a is taken immediately

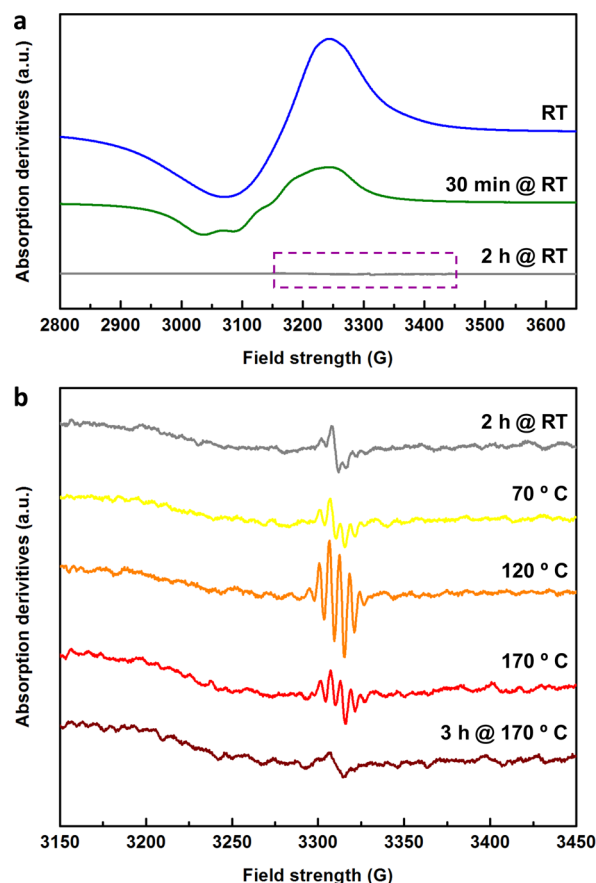


**Figure 3.** (a) In situ EPR response of the reactants at RT. From the top, the figure shows the reactants' EPR signals upon mixing (blue), after 30 min at RT (green), and 2 h after RT (gray). (b) EPR signals of the reaction during heating. From the top, the figure shows the EPR spectra of the reaction before heating (gray, the enlarged purple area in panel a), at 70 °C (yellow), at 120 °C (orange), at 170 °C (red), and 3 h at 170 °C (wine).

after the reactants are mixed at RT. A broad EPR signal centering at 3165 G ( $g$ -factor, or  $g = 2.09559$ ) is observed. This strong and broad feature can be assigned to Cu(II) species which originated from Cu losing two electrons, and taking the 3d<sup>9</sup> electron configuration, rendering one unpaired electron.<sup>16</sup> The absence of subtle features is due to line broadening caused by strong dipolar interactions.<sup>17</sup> This broadening is commonly observed in concentrated solution.<sup>18</sup> After 30 min at RT the broad feature (green), preserves its general centering position but with intensity visibly reduced. In addition, subtle patterns are resolved due to lowered concentration. After 2 h, the Cu(II) pattern is undetectable (gray). Coupled with the disappearance of the signature blue color, we believe that Cu(II) is completely



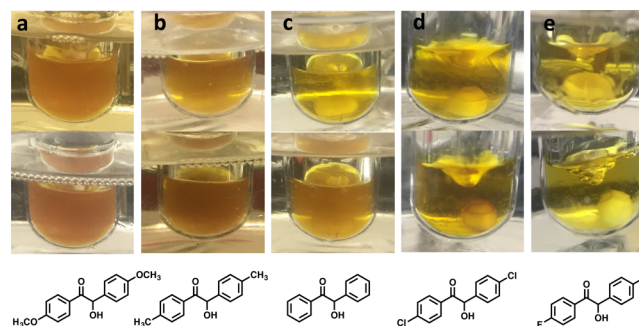
reduced to Cu(I) species at this stage (Figure S2a,b). A control experiment without benzoin shows no change in the spectra at RT, indicating that benzoin, rather than oleylamine reduces Cu(II) to Cu(I) (Figure S3).

Figure 3b keeps track of the EPR response during the heating of the reaction solution. Sharp features with  $g$  factor calculated as 2.00331 are observed. EPR lines with  $g$ -value close to 2, correspond to a free radical signal,<sup>18</sup> which we believe is produced by the thermal decomposition of benzoin. In the first spectrum (enlarged purple area of Figure 3a), taken at RT, a sharp radical-like feature is already resolved. This echoes the observation of room-temperature reduction of Cu(II) complex. It indicates that, without heating, benzoin is already slowly decomposing and producing radicals. This decomposition, even though slow, can already build up a steady-state concentration which can be detected by EPR spectroscopy. The radicals produced have efficient reducing power to reduce Cu(II) to Cu(I) but no further, likely due to the low concentration.

As the temperature reaches 70 °C, the radical signal becomes stronger (yellow). Evidently as temperature is increased, the decomposition of benzoin become faster, and the concentration of radicals also increases. As the reaction temperature goes up to 120 °C, reddish copper product starts to precipitate out in the EPR tubes. The EPR signal (orange) becomes stronger. The asymmetric shape of the EPR spectrum infers that there are multiple radical species present in the sample, causing superposition of lines with different  $g$ -values.<sup>18</sup> The spectrum of the primary radicals in the system has six well resolved hyperfine lines. The absence of one intense central line suggests that there exist an odd number of equivalent hydrogens contributing to hyperfine coupling.<sup>18</sup> The spectrum obtained here does not match with previously reported data for low temperature (<100 K) benzoyl (three lines with one strong center),<sup>19</sup> nor  $\alpha$ -hydroxybenzyl radical (evenly distributed 21 lines<sup>20</sup>). Owing to the high-temperature enhanced line shift/broadening effect,<sup>17b</sup> a full interpretation of this spectrum is not straightforward. One possible explanation is that at high temperature, benzoyl radicals ( $\sigma$ -radical) resonance into its  $\pi$ -isomer (Figure S4).<sup>21</sup> The energy barrier of this transformation is easily overcome by thermal input and thus comparable amounts of both species exist under the reaction conditions.<sup>22</sup> Further studies are needed to elucidate the exact reaction mechanism.

As the temperature continues to increase, more copper product emerges from the tube. Meanwhile, the radical signal (red) decreases due to the consumption of the material. Then, the solution was left to react at 170 °C for 3 h, and the additional EPR spectra at 170 °C with different time intervals is shown Figure S5. The radical signals keep declining as the reaction goes on. It is worth noting that the radicals are not instantly consumed even at this high temperature. Rather, the radical signals are still strong after 30 min's reaction, and well resolved even after 1.5 h of heating. This indicates that the radicals have a long enough lifetime to build up a detectable concentration at high temperature for several hours. And the long-lasting radicals serve as the active reducing agent throughout the entire reaction. However, the long maintained radical signal level does not necessarily point to ultrastable radical species. This equilibrium concentration is balanced by benzoin's decomposition and radical consumption. In the final spectrum (wine), the radical signal is barely resolved. Copper metal can be observed within the EPR tube (Figure S2c).

The reactivity of benzoin can be tuned by introducing electron-donating/electron-withdrawing groups on the benzoin molecule. We find that, with electron-donating group as substitution, the reducing power is largely promoted; while electron-withdrawing substitution diminishes benzoin's reduction reactivity. Figure 4 shows the series of control experiments



**Figure 4.** Pictures of different stages of Cu NWs synthesis using (a) 4,4-dimethoxybenzoin, (b) 4,4-dimethylbenzoin, (c) benzoin, (d) 4,4'-dichlorobenzoin, and (e) 4,4'-difluorobenzoin as reducing agents. The upper and middle panels show the pictures of reactions run for 1 and 2 h, respectively; the lower panel shows the chemical structures used in corresponding reactions. The reactions were all carried out at 180 °C.

carried out to test the reactivity of different benzoin derivatives. When the mixtures are heated at 180 °C for 1 h, a large amount of copper is already reduced out using dimethoxybenzoin as reducing agent, as compared to the smaller amount in the case of dimethylbenzoin, and there is no visible copper species in the case of benzoin, dichlorobenzoin, and difluorobenzoin. Two hours into the reaction, the production of copper follows the same trend, in which the electron donating modification promotes the reaction while the electron withdrawing case suppresses the reduction. The yields of copper product after a 3 h reaction time are measured to be 94.0%, 65.3%, 31.3%, 2.5%, and 0% for reactions with 4,4'-dimethoxybenzoin, 4,4'-dimethylbenzoin, benzoin, 4,4'-dichlorobenzoin, and 4,4'-difluorobenzoin, respectively. The TEM images of the products are shown in Figure S6. The substitutes may either modify the carbon-carbon bond cleavage energy or the redox potential of the resulting free radicals, and these modifications eventually change the reactivity of the radicals.

Additionally, benzoin is compatible with both hydrophilic and hydrophobic solvent systems. This gives it great potential as generalized reducing agents in the broader nanomaterial syntheses. For example, colloidal synthesis of silver NWs is only possible when (polyvinylpyrrolidone) PVP, a hydrophilic surfactant, is used as shaping ligands. Benzoin can be readily used as a reducing agent for silver NW syntheses as well. Silver nitrate can be reduced to silver metal by benzoin at 130 °C. The NW formation undertakes a similar mechanism as copper. Ag(0) tend to nucleate to 5-fold-twinned seeds in the presence of PVP and then grow to one-dimensional NWs. A control experiment without the addition of benzoin shows no silver ion reduction at the same temperature, giving evidence to benzoin's role of reducing agent. The resulting silver NWs have a mean diameter of 50 nm as shown in Figure 5a. Ultrathin gold NWs, shown in Figure 5b, can also be synthesized using benzoin as reducing agent in the presence of oleylamine. The average diameter of as-grown gold NWs is around 3 nm.

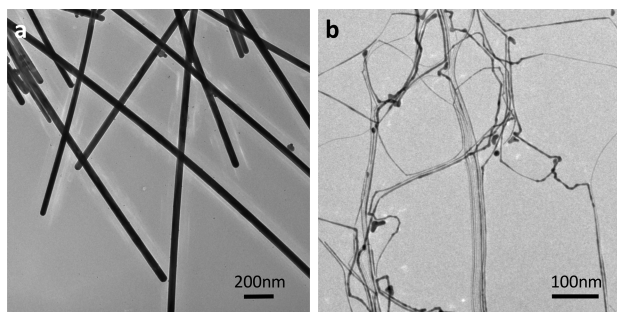


**Figure 5.** TEM images of as-grown (a) silver and (b) gold NWs using benzoin as reducing agent.

## CONCLUSIONS

In summary, we demonstrate a new synthetic approach that used benzoin and its derivatives as reducing agent to grow high quality Cu NWs. The active species during the reduction are attributed to the free radicals produced via thermal decomposition of benzoin. The reaction mechanism was studied using in situ temperature-dependent EPR spectroscopy. Reduction of copper is observed in line with evolution of free radicals. Furthermore, benzoin is shown to have a wide tunability of reducing powers by changing its substitution derivatives. These unique features make benzoin and its derivatives useful in metal nanowire growth and also open up new opportunities for the broader nanomaterial synthesis.

## EXPERIMENTAL SECTION

**Synthesis of Copper NWs.** In a typical reaction, 85 mg of  $\text{CuCl}_2 \cdot \text{H}_2\text{O}$  (0.5 mmol), and 5 g of oleylamine were mixed in a reaction vessel. The mixture was sonicated at room temperature until it became a clear blue solution. Then, 0.424 g of benzoin was added in the solution. The mixture was then degassed and purged with nitrogen at 70 °C for 30 min. Next, the reaction temperature was raised to 120 °C under  $\text{N}_2$  atmosphere and kept for approximately 20 min until the color of the solution reached clear yellow. Next, the temperature was raised to 185 °C and was kept at that temperature for 3 h until the reaction was complete. The product was harvested by centrifugation at 8000 rpm for 5 min. Then, the NWs were washed with toluene, and then toluene/isopropyl alcohol (1:1) three times to remove excess oleylamine and benzoin for further characterizations.

**Synthesis of Ag and Gold NWs Using Benzoin.** To synthesize silver NWs, 0.15 M polyvinylpyrrolidone (PVP, Mw ~ 55 000) and 0.1 M  $\text{AgNO}_3$  solution in ethylene glycol were prepared in advance. Benzoin (2 mmol) was dissolved in ethylene glycol and the solution was purged with  $\text{N}_2$  to remove oxygen. Then, the benzoin solution was slowly heated up to 130 °C under argon protection. A 3 mL aliquot of PVP solution and 3 mL of  $\text{AgNO}_3$  solution were simultaneously injected in a dropwise fashion. Next, the reactants were left to react for 10 min before being ramped up to 140 °C where the mixture was left for an extra hour. The product was harvested by centrifuging, and it was washed 3 times with isopropyl alcohol. To synthesize gold NWs, 0.3 mg of oleylamine, 22 mg of  $\text{HAuCl}_4$ , and 8.77 mg of benzoin were dissolved in 13 g of hexanes under vigorous stirring. After the solution was clear, the mixture was left undisturbed at room temperature for 5 h. The product was collected by centrifuging and washed 3 times with toluene.

**Preparation of Benzoin Derivatives.**<sup>23</sup> 4,4'-Dichlorobenzoin and 4,4'-difluorobenzoin are synthesized using a documented approach: 20 mmol 4-chlorobenzaldehyde (or 4-fluorobenzaldehyde), 1 mmol 1,3-dimethylbenzimidazolium, and 1 mL of 1,8-diazabicyclo[7.1.1]undec-7-ene were dispersed in 50 mL of tetrahydrofuran. The mixture was heated up to 66 °C and gently refluxed under a  $\text{N}_2$  environment for 12 h. Then the solution was cooled to room temperature and was concentrated by evaporation of solvent under

reduced pressure using a rotovap. The residue was purified using column chromatography (chloroform and hexanes as eluent) to remove unreacted precursors and side products. The final product benzoin was extracted from the evaporation of solvents and dried in a vacuum oven overnight before use.

**Benzoin Reactivity Tuning.** Five types of benzoin were set to compare their reducing power in the copper NW synthesis reaction. The five benzoin are 4,4'-dimethoxybenzoin, 4,4'-dimethylbenzoin, benzoin, 4,4'-dichlorobenzoin, and 4,4'-difluorobenzoin. In each of the five reactions, 0.5 mmol  $\text{CuCl}_2 \cdot \text{H}_2\text{O}$  (0.5 mmol), 2 mmol benzoin of one type, and 5 g of oleylamine were mixed in a reactor. Then the mixture went through the same heating steps as described before and was kept at 175 °C for the same amount of time. Pictures of the reaction progress were taken at 1 and 2 h into the reaction. All reactions were stopped at 3 h. The products were harvested through centrifuge. No extra washing steps were carried out to preserve the products as much as possible. Then, the collected materials were dispersed in toluene and vacuum filtered on to a nitrocellulose membrane. The copper products on filter membrane were dried in a vacuum oven and weighed for yield calculation.

**Characterizations of Metal NWs.** The morphology of synthesized product was examined using transmission electron microscope (TEM) and scanning electron microscope (SEM, JEOL JSM-6340F). Lower-resolution TEM images were acquired using a Hitachi H7650 instrument, operated at 100 kV, and higher-resolution TEM characterizations were carried out on a FEI Tecnai G20 instrument, with a high voltage set at 200 kV. X-ray diffraction (XRD) was acquired using a Bruker D-8 General Area Detector Diffraction System (GADDS) with HI-STAR area charge-coupled device (CCD) detector, equipped with a Co  $K\alpha$  source ( $\lambda = 1.789 \text{ \AA}$ ).

**In Situ Electron Paramagnetic Resonance (EPR) Measurement.** The EPR sample was prepared in airtight EPR tubes (4 mm LPV 250 mm EPR sample tube) purchased from Wilmad LabGlass. All sample tubes were cleaned with acetone and isopropyl alcohol under ultrasonication and then dried in a heated oven before use.

Before loading the sample in EPR tubes, the benzoin and  $\text{CuCl}_2$  solution was prepared freshly right before the measurement. Benzoin was dispersed in oleylamine under vigorous stirring with a concentration of 0.8 mmol/g.  $\text{CuCl}_2$  oleylamine solution with a concentration of 0.02 mmol/g was prepared. In a standard reaction sample preparation, 75  $\mu\text{L}$  of 0.8 mmol/g benzoin oleylamine mixture was added to the EPR tube with gentle shaking. Then 75  $\mu\text{L}$  of  $\text{CuCl}_2$  solution was added on top of the mixture in the tube. The tube was shaken back and forth until the solution was well mixed and settled to the bottom. The loaded EPR tube was connected to a Schlenk line then degassed and purged with argon for five cycles and finally sealed with slight vacuum before going through the measurement.

The EPR measurement was conducted on a Bruker EMXplus EPR spectrometer. The microwave frequency was set at 9.286 GHz with a power of 20 mW. For the measurement of Cu(II) complex signals, the center field was kept at 3200G, with a sweep width of 1000G. In the measurement targeting radical signals, the field was centered at 3300G with a sweep width being 300G. Each spectrum was integrated from 60 or 15 scans. The freshly made sample tube was inserted in the measurement chamber and then put through different temperatures that mimic the Schlenk tube reaction conditions. Spectra were collected at appropriate temperatures and time intervals: ~1 min at room temperature (RT), 30 min at RT, 2 h at RT, 30 min at 70 °C, 30 min at 120 °C, 30 min at 170 °C, and finally 3 h at 170 °C. All spectra were collected from one sample, and the EPR tube was kept sealed under vacuum throughout the measurement.

## ASSOCIATED CONTENT

### Supporting Information

The Supporting Information is available free of charge on the ACS Publications website at DOI: 10.1021/jacs.6b11900.

Experimental details, additional TEM images, EPR spectra (PDF)

## ■ AUTHOR INFORMATION

## Corresponding Author

\*p\_yang@berkeley.edu

ORCID 

Fan Cui: 0000-0003-3394-8095

Peidong Yang: 0000-0003-4799-1684

## Notes

The authors declare no competing financial interest.

## ■ ACKNOWLEDGMENTS

The authors gratefully thank Dr. B. Wu and Prof. G. Stucky for the facility support at UC Santa Barbara, Dr. R. Larson for the help in the benzoin derivative syntheses, Prof. K. Lakshmi for helpful discussion in EPR measurements and Ms. C. Xie for proof reading. We also thank Dr. S. Walker for the help with the in situ EPR studies at the Materials Research Laboratory, UC Santa Barbara. The MRL Shared Experimental Facilities are supported by the MRSEC Program of the NSF under Award No. DMR 1121053; a member of the NSF-funded Materials Research Facilities. Work at the NCEM, Molecular Foundry was supported by the Office of Science, Office of Basic Energy Sciences, of the U.S. Department of Energy under Contract No. DE-AC02-05CH11231. This work was financially supported by BASF Corporation (Funding No. 84428967).

## ■ REFERENCES

- (1) Hsu, P.-C.; Wang, S.; Wu, H.; Narasimhan, V. K.; Kong, D. S.; Lee, H. R.; Cui, Y. *Nat. Commun.* **2013**, *4*, 2522.
- (2) (a) Tao, A.; Kim, F.; Hess, C.; Goldberger, J.; He, R.; Sun, Y.; Xia, Y.; Yang, P. *Nano Lett.* **2003**, *3*, 1229. (b) Sanders, A. W.; Routenberg, D. A.; Wiley, B. J.; Xia, Y.; Dufresne, E. R.; Reed, M. A. *Nano Lett.* **2006**, *6*, 1822.
- (3) Liang, H. W.; Cao, X.; Zhou, F.; Cui, C. H.; Zhang, W. J.; Yu, S. H. *Adv. Mater.* **2011**, *23*, 1467.
- (4) Kim, K. K.; Hong, S.; Cho, H. M.; Lee, J.; Suh, Y. D.; Ham, J.; Ko, S. H. *Nano Lett.* **2015**, *15*, 5240.
- (5) (a) Dou, L.; Cui, F.; Yu, Y.; Khanarian, G.; Eaton, S. W.; Yang, Q.; Resasco, J.; Schildknecht, C.; Schierle-Arndt, K.; Yang, P. *ACS Nano* **2016**, *10*, 2600. (b) Hu, L.; Kim, H. S.; Lee, J.; Peumans, P.; Cui, Y. *ACS Nano* **2010**, *4*, 2955. (c) De, S.; Higgins, T. M.; Lyons, P. E.; Doherty, E. M.; Nirmalraj, P. N.; Blau, W. J.; Boland, J. J.; Coleman, J. N. *ACS Nano* **2009**, *3*, 1767.
- (6) (a) Ye, E.; Zhang, S.; Liu, S.; Han, M. *Chem. - Eur. J.* **2011**, *17*, 3074. (b) Yang, H.; He, S.-Y.; Tuan, H.-Y. *Langmuir* **2014**, *30*, 602.
- (7) (a) Mohl, M.; Pusztai, P.; Kukovecz, A.; Konya, Z.; Kukkola, J.; Kordas, K.; Vajtai, R.; Ajayan, P. M. *Langmuir* **2010**, *26*, 16496. (b) Jin, M.; He, G.; Zhang, H.; Zeng, J.; Xie, Z.; Xia, Y. *Angew. Chem., Int. Ed.* **2011**, *50*, 10560.
- (8) (a) Zhang, X.; Zhang, D.; Ni, X.; Zheng, H. *Solid State Commun.* **2006**, *139*, 412. (b) Wang, W.; Li, G.; Zhang, Z. *J. Cryst. Growth* **2007**, *299*, 158.
- (9) (a) Chang, Y.; Lye, M.; Zeng, H. *Langmuir* **2005**, *21*, 3746. (b) Rathmell, A. R.; Wiley, B. J. *Adv. Mater.* **2011**, *23*, 4798. (c) Meng, F.; Jin, S. *Nano Lett.* **2012**, *12*, 234.
- (10) (a) Zhang, D.; Wang, R.; Wen, M.; Weng, D.; Cui, X.; Sun, J.; Li, H.; Lu, Y. *J. Am. Chem. Soc.* **2012**, *134*, 14283. (b) Guo, H.; Lin, N.; Chen, Y.; Wang, Z.; Xie, Q.; Zheng, T.; Gao, N.; Li, S.; Kang, J.; Cai, D.; Peng, D. *Sci. Rep.* **2013**, *3*, 2323.
- (11) Cui, F.; Yu, Y.; Dou, L.; Sun, J.; Yang, Q.; Schildknecht, C.; Schierle-Arndt, K.; Yang, P. *Nano Lett.* **2015**, *15*, 7610.
- (12) Meng, F.; Morin, S. A.; Forticaux, A.; Jin, S. *Acc. Chem. Res.* **2013**, *46*, 1616.
- (13) Fouassier, J. P. *Photoinitiation, Photopolymerization and Photocuring*; Hanser Verlag: Munich, 1995.
- (14) Itakura, T.; Torigoe, K.; Esumi, K. *Langmuir* **1995**, *11*, 4129.

- (15) Lewis, F. D.; Lauterbach, R. T.; Heine, H. G.; Hartmann, W.; Rudolph, H. *J. Am. Chem. Soc.* **1975**, *97*, 1519.
- (16) Comba, P.; Hambley, T. W.; Hitchman, M. A.; Stratemeier, H. *Inorg. Chem.* **1995**, *34*, 3903.
- (17) (a) Ito, M. *J. Chem. Phys.* **1965**, *42*, 391. (b) Bales, B.; Peric, M. *J. Phys. Chem. A* **2002**, *106*, 4846.
- (18) Gerson, F.; Huber, W. *Electron Spin Resonance Spectroscopy of Organic Radicals*; Wiley-VCH: Weinheim, Germany, 2003.
- (19) Wilson, R. J. *Chem. Soc. B* **1968**, *0*, 84.
- (20) Krusic, P. J.; Rettig, T. A. *J. Am. Chem. Soc.* **1970**, *92*, 722.
- (21) Dewar, M. J. S.; Kirschner, S.; Kollmar, H. W.; Wade, L. E. *J. Am. Chem. Soc.* **1974**, *96*, 5242.
- (22) Davidson, R. S.; Edwards, J.; Warburton, S. K. *J. Chem. Soc., Perkin Trans. 1* **1976**, 1511.
- (23) Miyashita, A.; Suzuki, Y.; Iwamoto, K.; Higashino, T. *Chem. Pharm. Bull.* **1994**, *41*, 2633.